

RESEARCH ARTICLE | OCTOBER 24 2024

Optimal synchronization to a limit cycle

C. Ríos-Monje ; C. A. Plata ; D. Guéry-Odelin ; A. Prados  



Chaos 34, 103146 (2024)

<https://doi.org/10.1063/5.0227287>



Chaos

Special Topics Open
for Submissions

[Learn More](#)



Optimal synchronization to a limit cycle

Cite as: Chaos 34, 103146 (2024); doi: 10.1063/5.0227287

Submitted: 8 July 2024 · Accepted: 9 October 2024 ·

Published Online: 24 October 2024



View Online



Export Citation



CrossMark

C. Ríos-Monje,¹ C. A. Plata,¹ D. Guéry-Odelin,^{2,3} and A. Prados^{1,a)}

AFFILIATIONS

¹Física Teórica, Universidad de Sevilla, Apartado de Correos 1065, E-41080 Sevilla, Spain

²Laboratoire Collisions, Agrégats, Réactivité, FeRMI, Université Toulouse III—Paul Sabatier, 118 Route de Narbonne, 31062 Toulouse Cedex 09, France

³Institut Universitaire de France, 1 Rue Descartes, 75231 Paris Cedex 05, France

^{a)}Author to whom correspondence should be addressed: prados@us.es

ABSTRACT

In the absence of external forcing, all trajectories on the phase plane of the van der Pol oscillator tend to a closed, periodic trajectory—the limit cycle—after infinite time. Here, we drive the van der Pol oscillator with an external time-dependent force to reach the limit cycle in a given finite time. Specifically, we are interested in minimizing the non-conservative contribution to the work when driving the system from a given initial point on the phase plane to any final point belonging to the limit cycle. There appears a speed-limit inequality, which expresses a trade-off between the connection time and cost—in terms of the non-conservative work. We show how the above results can be generalized to the broader family of non-linear oscillators given by the Liénard equation. Finally, we also look into the problem of minimizing the total work done by the external force.

Published under an exclusive license by AIP Publishing. <https://doi.org/10.1063/5.0227287>

Self-sustained oscillations are relevant not only in physics—e.g., in electronics, lasers, or active matter—but also in many other contexts: neuroscience, physiology, and economics, to name just a few.^{1,2} A key feature of self-oscillatory systems is the existence of a stable limit cycle, which appears as a consequence of the non-linearity of the damping force. The limit cycle is stable because neighboring trajectories approach it in the long-time limit, i.e., after a certain typical relaxation time t_R . Here, importing ideas from the field of shortcuts to adiabaticity in quantum mechanics³ and swift state-to-state transformations (SSTs) in classical and stochastic systems,⁴ we address the problem of shortcutting the relaxation to the limit cycle by driving the system with a suitable external force during a given time $t_f < t_R$. Specifically, we aim at building a SST that minimizes the non-conservative work. The emergence of a speed-limit inequality is shown, with a trade-off between the connection time and the non-conservative work. This inequality entails that, for small damping, when the natural relaxation time of the system to the limit cycle is very long, the relaxation to the limit cycle can be accelerated by a very large factor while keeping the energetic cost finite. Interestingly, the developed framework for the van der Pol oscillator naturally extends to the more general case of the Liénard equation, with tiny changes. In addition, the minimization of the total work, including both the conservative and non-conservative contributions, is investigated.

I. INTRODUCTION

Stable limit cycles appear in systems that show oscillatory behavior in the long-time limit without any time-periodic driving. In other words, limit cycles correspond to self-sustained oscillations, which are present in a wide variety of non-linear systems. In physics, self-sustained oscillations in non-linear circuits were the motivation for van der Pol's pioneering work⁵ (see Ref. 1 for a review). More currently, they are being investigated in the field of active matter.^{6–10} In addition, self-oscillations are often found in biological systems; for example, they have been shown to be relevant for circadian rhythms^{11,12} or the migration of cancer cells in confined environments.¹³

The van der Pol equation is a paradigmatic model for self-sustained oscillations. In dimensionless variables, it reads

$$\ddot{x} + \mu(x^2 - 1)\dot{x} + x = 0, \quad (1)$$

where $\mu > 0$ is a parameter, to which we will refer as the damping constant. Variations in the van der Pol equation have been employed in many fields, e.g., to electronically simulate nerve axons,^{14,15} to understand the dynamics of elastic excitable media,¹⁶ or to model self-sustained oscillations in active matter.¹⁷ The undriven van der Pol oscillator takes an infinite time to reach the limit cycle, with a relaxation time that decreases with the damping constant μ . For

small damping $\mu \ll 1$, the natural relaxation time t_R to the limit cycle is very long, $t_R = O(\mu^{-1})$.¹⁸

Only very recently,¹⁹ the problem of accelerating the relaxation to the limit cycle has been addressed, in the context of the SST recently introduced in classical and stochastic systems.⁴ The general idea of the SST, which is rooted in the field of quantum shortcuts to adiabaticity,³ is to introduce a suitable driving to make the system reach the desired target state in a time shorter than the natural relaxation time. Still, neither the energetic cost of such an acceleration nor the physical implications thereof have been investigated for the synchronization to a limit cycle.

In this work, we aim at investigating the energetic cost of driving the van der Pol oscillator to its limit cycle in a finite time. More specifically, we are interested in engineering an optimal driving $F(t)$ —to be added to the right-hand side (rhs) of Eq. (1)—that minimizes the dissipative work done by the non-conservative non-linear force $F_{nc}(x, \dot{x}) \equiv -\mu(x^2 - 1)\dot{x}$. This problem has strong similarities with the minimization of the irreversible work in stochastic systems,^{4,20–23} although the van der Pol oscillator is not coupled to a heat bath. In addition, it raises the question of the trade-off between operation time and cost, as measured by the non-conservative work, and the possible emergence of speed limit inequalities.^{4,24–38}

The minimization of the non-conservative work is carried out by considering that the system starts from a given point on the phase plane and reaches any point of the limit cycle in a given connection time t_f —ideally, much shorter than the natural relaxation time t_R . When the force is not bounded, which is the case we address in this paper, this minimization problem can be tackled with the tools of variational calculus, incorporating the variable end point via the so-called transversality condition.^{39,40} Remarkably, our analysis shows that many of the results, including the optimal end point over the limit cycle, can be obtained without having to know the explicit expression for the limit cycle.

In this work, we also consider possible generalizations of the above problem. First, we will show that practically all results found for the minimization of the non-conservative work in the van der Pol case extend, with tiny changes, to the Liénard equation—which is a model that covers a much broader family of oscillators, including van der Pol's as a particular case. Second, we will tackle the minimization of the total work done by the external force, including both the conservative and non-conservative contributions.

The structure of the paper is as follows. Section II presents the model and some basic equations that we need for our analysis. In Sec. III, we carry out the minimization of the non-conservative work. We derive the Euler–Lagrange equations for the optimal path in phase space in Sec. III A. Therefrom, we obtain explicit expressions for the optimal path and force in Sec. III B. The transversality condition for the variable end point problem is analyzed in Sec. III C. Using the results of Secs. III A–III C, the explicit expression for the minimum non-conservative work is derived in Sec. III D. We illustrate our results and discuss their physical implications in Sec. III E. Section IV is devoted to generalizing our results to more complex scenarios: the Liénard equation in Sec. IV A and the minimization of the total work in Sec. IV B. Finally, we present the main conclusions of our work and some perspectives for further research in Sec. V.

II. MODEL

As anticipated in Sec. I, we are interested in investigating the van der Pol oscillator driven by an external force $F(t)$,

$$\ddot{x} + \mu(x^2 - 1)\dot{x} + x = F(t), \quad (2)$$

to accelerate the relaxation toward the limit cycle, which is described by an implicit function of (x, \dot{x}) that also depends on the parameter μ , $\chi_{\ell c}(x, \dot{x}; \mu) = 0$. In the following, we refer to Eq. (2) as the driven van der Pol equation (dvdPE). For our purposes, it is convenient to explicitly introduce the phase plane point as

$$\mathbf{x}(t) \equiv (x_1(t), x_2(t)), \quad x_1 \equiv x, \quad x_2 \equiv \dot{x}, \quad (3)$$

and rewrite the dvdPE (2) as a system of first-order differential equations,

$$\dot{\mathbf{x}} = \begin{pmatrix} x_2 \\ -\mu(x_1^2 - 1)x_2 - x_1 + F \end{pmatrix} \equiv \mathbf{f}(\mathbf{x}; F), \quad (4)$$

i.e.,

$$\dot{x}_1 = f_1(x_2) \equiv x_2, \quad (5a)$$

$$\dot{x}_2 = f_2(x_1, x_2; F) \equiv -\mu(x_1^2 - 1)x_2 - x_1 + F. \quad (5b)$$

Note that, in order to simplify our notation, we have omitted the time dependence in both in phase-space variables $(x_1(t), x_2(t))$ and in force $F(t)$.

We would like to reach the limit cycle by applying the driving force $F(t)$ for a given finite time t_f . That is, we want to drive the system from a given initial state (x_{10}, x_{20}) , to a final end point of the limit cycle, i.e., (x_{1f}, x_{2f}) , with $\chi_{\ell c}(x_{1f}, x_{2f}; \mu) = 0$, in a finite time t_f . Once the limit cycle is reached at $t = t_f$, the force is switched off, i.e., $F(t) = 0$ for $t \geq t_f$, so that the system remains over the limit cycle $\forall t \geq t_f$.

We aim at optimizing the energetic cost of the driving described above. Bringing to bear the dvdPE (2) [or (4)], the work done on the system by the external force $F(t)$ can be split into a conservative part $\Delta E = E_f - E_0$, which only depends on the initial and final points on the phase plane, and a non-conservative part W_{nc} , which depends on the whole trajectory of the system,

$$W \equiv \int_0^{t_f} dt F(t) \dot{x}(t) = \Delta E + W_{nc}, \quad (6)$$

with

$$E(\mathbf{x}) \equiv \frac{1}{2}(x_1^2 + x_2^2), \quad W_{nc}[\mathbf{x}] \equiv \mu \int_0^{t_f} dt (x_1^2 - 1)x_2^2. \quad (7)$$

Although the oscillator is not explicitly coupled to a heat bath, if we interpret E as the internal energy of the oscillator, W_{nc} would be the heat dissipated to the environment due to the non-linear friction force.⁴¹ In the following, we will mainly be interested in the minimization of the non-conservative contribution to the work. This

minimization has to be done with the boundary conditions,

$$x_1(0) = x_{10}, x_2(0) = x_{20}, x_1(t_f) = x_{1f}, x_2(t_f) = x_{2f}, \quad (8a)$$

$$\chi_{\ell c}(\mathbf{x}_f; \mu) = 0; \quad (8b)$$

the latter condition enforces that \mathbf{x}_f belongs to the limit cycle. In the following, it will be useful to introduce the maximum amplitude $x_{\ell c}^{\max}$ of oscillation over the limit cycle.

We remark the formal similarity of our minimization problem with the minimization of the irreversible work in systems with stochastic dynamics.^{4,21–23,42} Therein, the total work may be split into two contributions: (i) the free energy difference ΔF , which is given by the initial and final equilibrium points (the analogous role here is played by ΔE), and (ii) the irreversible work, which is a functional of the trajectory, and it is positive definite (the analogous role here is played by W_{nc}). Still, two key differences should be remarked: here, (i) the sign of W_{nc} is not necessarily positive, due to the change in the sign of the non-linearity at $|x_1| = 1$, which, in turn, is responsible for the emergence of a limit cycle, and (ii) the final point is not fixed, since we would like to join the initial point to any point of the limit cycle.⁴³

For an arbitrary value of the damping coefficient μ , there is neither a closed analytical expression for the function $\chi_{\ell c}(x_1, x_2; \mu) = 0$ defining implicitly the limit cycle nor a closed analytical expression for the relaxation of the system toward it. Yet, in the small damping limit $\mu \ll 1$, a multiple scale analysis of Eq. (1) gives asymptotically valid expressions for both $\chi_{\ell c}$ and the time evolution $\mathbf{x}(t)$ toward the long-time behavior—e.g., see Ref. 18. Specifically, one has

$$\chi_{\ell c} \sim x_1^2 + x_2^2 - 4 + O(\mu), \quad (9a)$$

$$x_1(t) \sim 2 \left(1 - \frac{r_0^2 - 4}{r_0^2} e^{-\mu t} \right)^{1/2} \cos(t + \phi_0) + O(\mu), \quad (9b)$$

$$x_2(t) \sim -2 \left(1 - \frac{r_0^2 - 4}{r_0^2} e^{-\mu t} \right)^{1/2} \sin(t + \phi_0) + O(\mu), \quad (9c)$$

where

$$r_0 = \sqrt{x_{10}^2 + x_{20}^2}, \quad \phi_0 = \arctan \frac{x_{20}}{x_{10}}. \quad (10)$$

For $\mu \ll 1$, the maximum amplitude of the limit cycle approaches 2,

$$\tilde{x}_{\ell c}^{\max} \equiv \lim_{\mu \rightarrow 0^+} x_{\ell c}^{\max} = 2. \quad (11)$$

The value of $\tilde{x}_{\ell c}^{\max}$ stems from the multiple scale expression in Eq. (9b). In addition, a physical argument could be given as follows: for $\mu = 0$, circular orbits with $x_1 = A \cos(t + \phi_0)$, $x_2 = -A \sin(t + \phi_0)$, for any A are possible. For $\mu \ll 1$, this is no longer the case: the only possible circular orbit must have a vanishing non-conservative work, as given by Eq. (7), over the circumference: this gives $A = 2$. On the one hand, it has been shown that $x_{\ell c}^{\max}$ has a very weak dependence on μ , being very close to $\tilde{x}_{\ell c}^{\max} = 2$ for all μ , namely, $2 \leq x_{\ell c}^{\max} \leq 2.0672$.⁴⁴ On the other hand, the shape of the limit cycle strongly deviates from a circumference as μ increases.¹⁸

For small damping, $\mu \ll 1$, the relaxation time of the system t_R to the limit cycle is very long, of the order of μ^{-1} . Specifically, we

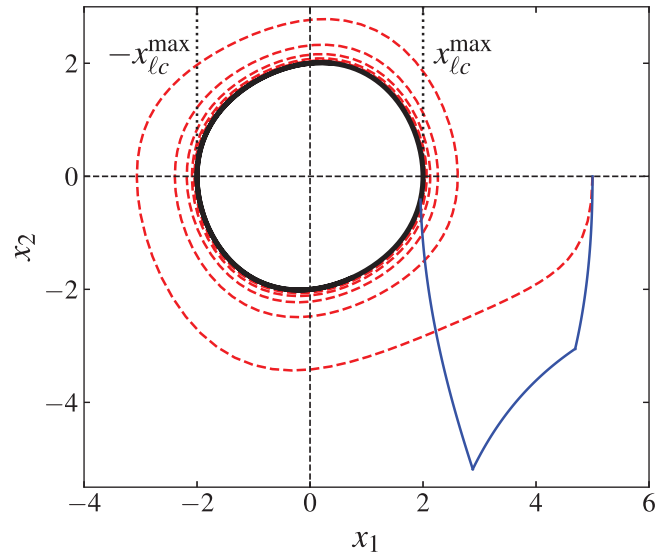


FIG. 1. Illustration of a free trajectory and a driven trajectory on the phase plane ($x_1 = x, x_2 = \dot{x}$) of the van der Pol oscillator with $\mu = 10^{-1}$. The thick line stands for the limit cycle of the system. Over the limit cycle, $-x_{\ell c}^{\max} \leq x_1 \leq x_{\ell c}^{\max}$; note that the van der Pol equation is symmetrical under point reflection with respect to the origin, i.e., $(x_1, x_2) \rightarrow (-x_1, -x_2)$. Also plotted are the vertical lines $x_1 = \pm x_{\ell c}^{\max}$ (dotted). The free trajectory (dashed red) reaches the limit cycle in an infinite time, whereas the driven trajectory (solid blue) reaches it in a finite time; here, $t_f = 1$. The plotted data correspond to the numerical integration of the van der Pol equation.

estimate $t_R = 4\mu^{-1}$, for which $e^{-\mu t_R} \simeq 0.02$. In Fig. 1, we present a typical relaxation of the van der Pol oscillator to the limit cycle for $\mu = 0.1$, i.e., $t_R = 40$.

The small damping limit is especially relevant for building a SST to the limit cycle by introducing a suitable driving $F(t)$, because of the long-time scale of the natural relaxation. In the opposite limit of large damping, $\mu \gg 1$, the relaxation to the limit cycle is almost instantaneous in the undriven case (see, e.g., Sec. 7.5 of Ref. 18). Therefore, in the following, we mainly focus on the small damping limit $\mu \ll 1$.

III. MINIMIZATION OF THE NON-CONSERVATIVE WORK

We would like to minimize W_{nc} , which is a functional of the phase plane trajectory \mathbf{x} , as given by Eq. (7). We, thus, have a variational problem,

$$W_{nc}[\mathbf{x}] = \int_0^{t_f} dt L(\mathbf{x}), \quad L(\mathbf{x}) = \mu(x_1^2 - 1)x_2^2, \quad (12)$$

where $L(\mathbf{x}) = \mu(x_1^2 - 1)x_2^2$ is our “Lagrangian.” This is a variational problem with constraints: $\dot{x}_1 = f_1, \dot{x}_2 = f_2$, as given by Eq. (5). These dynamical constraints are incorporated to the minimization problem by introducing time-dependent Lagrange multipliers. Moreover, the variable end point belonging to the limit cycle is included

by considering the so-called transversality condition,^{39,40} (see also the Appendix).

A. Euler-Lagrange equation

We start from the phase-space formulation of the problem in Eqs. (4)–(8). The minimization problem of $W_{nc}[\mathbf{x}]$ is constrained by the evolution equation (5). This constrained minimization problem is equivalent to minimize, without constraints, the following functional:

$$J[\mathbf{x}, \mathbf{p}, F] = \int_0^{t_f} dt L^*(\mathbf{x}, \dot{\mathbf{x}}, \mathbf{p}, F), \tag{13}$$

where

$$L^*(\mathbf{x}, \dot{\mathbf{x}}, \mathbf{p}, F) = L(\mathbf{x}) + \mathbf{p} \cdot [\dot{\mathbf{x}} - \mathbf{f}(\mathbf{x}; F)] \tag{14}$$

is the new “Lagrangian,” and $\mathbf{p}(t) \equiv (p_1(t), p_2(t))$ are the Lagrange multipliers, which, henceforth, we refer to as the momenta. We employ the usual notation for the scalar product, $\mathbf{u} \cdot \mathbf{v} = u_1 v_1 + u_2 v_2$.

The optimal path must satisfy the Euler–Lagrange equations,

$$\frac{d}{dt} \left(\frac{\partial L^*}{\partial \dot{x}_i} \right) = \frac{\partial L^*}{\partial x_i}, \quad \frac{d}{dt} \left(\frac{\partial L^*}{\partial \dot{p}_i} \right) = \frac{\partial L^*}{\partial p_i}, \tag{15a}$$

$$\frac{d}{dt} \left(\frac{\partial L^*}{\partial \dot{F}} \right) = \frac{\partial L^*}{\partial F}, \tag{15b}$$

i.e.,

$$\dot{p}_1 = 2\mu x_1 x_2^2 + p_2(2\mu x_1 x_2 + 1), \tag{16a}$$

$$\dot{p}_2 = 2\mu(x_1^2 - 1)x_2 - p_1 + \mu p_2(x_1^2 - 1), \tag{16b}$$

$$\dot{x}_1 = x_2, \tag{16c}$$

$$\dot{x}_2 = -\mu(x_1^2 - 1)x_2 - x_1 + F, \tag{16d}$$

$$0 = p_2. \tag{16e}$$

Equations (16c) and (16d) are just the evolution equation (5). Equation (16e) tells us that $p_2(t) = 0, \forall t \in [0, t_f]$, so we infer that $\dot{p}_2(t) = 0$ for $t \in (0, t_f)$. Making use of Eq. (16b), we get

$$p_1 = 2\mu(x_1^2 - 1)x_2, \quad \forall t \in (0, t_f). \tag{17}$$

Taking the time derivative of this expression and bringing to bear Eqs. (16a) and (16c), we eliminate the momenta and obtain the Euler–Lagrange equation,

$$(x_1^2 - 1)\ddot{x}_1 + x_1\dot{x}_1^2 = 0, \tag{18}$$

which has to be fulfilled by the optimal path that minimizes the non-conservative work. We solve this equation with the boundary conditions for x_1 , i.e., for the position, $x_1(0) = x_{10}, x_1(t_f) = x_{1f}$.

At first sight, it may seem surprising that the boundary conditions for x_2 , i.e., for the velocity \dot{x} , do not appear in the minimization problem. Since $x_2 = \dot{x}_1$, once we have the solution of Eq. (18), we cannot tune the boundary conditions for x_2 ; the solution of the Euler–Lagrange equation will not verify the boundary condition for

the velocity, in general. However, this is not problematic: the finite jumps in the velocity at the initial and final times neither change the x values nor contribute to the non-conservative work. In other words, after solving the Euler–Lagrange equation (18), we introduce—if needed—the finite jumps in velocity at the initial and final times of magnitudes $x_2(0^+) - x_{20}$ and $x_{2f} - x_2(t_f^-)$, respectively, as explained in detail below, by means of impulsive forces.

The Euler–Lagrange equations only tell us that the solution is an extremum of the considered functional but not that it is indeed a minimum. In order to look into this issue, it is convenient to define the “Hamiltonian,”⁴⁵

$$H(\mathbf{x}, \mathbf{p}, F) = \dot{\mathbf{x}} \cdot \mathbf{p} - L^*(\mathbf{x}, \dot{\mathbf{x}}, \mathbf{p}, F) = \mathbf{p} \cdot \mathbf{f}(\mathbf{x}; F) - L(\mathbf{x}). \tag{19}$$

Since H is linear in F , the following necessary condition, known as the generalized Legendre–Clebsch condition, must hold:⁴⁶

$$\frac{\partial}{\partial F} \left[\frac{d^2}{dt^2} \left(\frac{\partial H(\mathbf{x}, \mathbf{p}; F)}{\partial F} \right) \right] \geq 0 \tag{20}$$

for having a minimum of the considered functional. For our problem of concern, i.e., the minimization of $W_{nc}(\mathbf{x})$, the generalized Legendre–Clebsch condition entails that

$$x_1^2 - 1 \geq 0. \tag{21}$$

The above condition, thus, restricts the solution of the minimization problem to live in the region of the phase plane for which $x_1^2 \geq 1$. Therefore, we restrict ourselves to the region $|x_1| \geq 1$ in the following: in particular, both $|x_{10}| \geq 1$ and $|x_{1f}| \geq 1$, with $\text{sgn}(x_{10}) = \text{sgn}(x_{1f})$. For any other case, the minimization problem would have no solution, since condition (21) would be impossible to meet at all times. In the case $|x_{10}| \leq 1$ and $|x_{1f}| \leq 1$, one could, if anything, maximize the non-conservative work. This is reasonable from a physical point of view, since the non-conservative force is dissipative for $|x_1| > 1$, whereas it is active (injects energy) for $|x_1| < 1$.

B. Optimal path and force

Equation (18) has a first integral of motion, which for $x_1^2 > 1$ can be written as

$$\dot{x}_1 \sqrt{x_1^2 - 1} = C_1, \tag{22}$$

where C_1 is a constant. We define

$$g(x) \equiv \frac{1}{2} \left[x\sqrt{x^2 - 1} - \log \left| x + \sqrt{x^2 - 1} \right| \right], \tag{23}$$

such that $g'(x) = \sqrt{x^2 - 1}$. Therefore, $g(x_1)$ monotonically increases with x_1 —recall that $x_1^2 > 1$. With this definition, the solution of Eq. (18) can be written as

$$g(x_1(t)) = C_1 t + C_0, \tag{24}$$

where C_0 is another constant. The constants C_1 and C_0 are calculated as functions of x_{10} and x_{1f} ,

$$C_0 = g(x_{10}), \quad C_1 = \frac{g(x_{1f}) - g(x_{10})}{t_f}, \tag{25}$$

which completes the solution for the optimal trajectory that minimizes the non-conservative work. The initial and final velocities

over the optimal trajectories $\dot{x}_1(0^+)$ and $\dot{x}_1(t_f^-)$ are obtained from Eq. (22),

$$x_2(0^+) = \dot{x}_1(0^+) = \frac{C_1}{\sqrt{1-x_{10}^2}}, \quad x_2(t_f^-) = \dot{x}_1(t_f^-) = \frac{C_1}{\sqrt{1-x_{1f}^2}}. \quad (26)$$

Note that, as already anticipated after Eq. (18), the velocity x_2 does not comply, in general, with the boundary conditions, but this is not problematic. We can introduce two impulsive contributions to the force—i.e., two delta peaks—at the initial and final times to fix this issue, neither changing the particle position nor performing any work.

Making use of the driven dvdPE (2), particularized for the optimal trajectory, we get the driving force,

$$F_{EL}(t) = -C_1^2 \frac{x_1(t)}{[x_1^2(t) - 1]^2} + \mu C_1 \sqrt{x_1^2(t) - 1} + x_1(t), \quad (27)$$

for $0^+ < t < t_f^-$. At $t = 0^+$ and $t = t_f^-$, the finite jumps in $x_2 = \dot{x}_1$ entail that $F(t)$ has delta peaks, at $t = 0^+$ and $t = t_f^-$, a behavior that has also been found in the optimization of the irreversible work done on a harmonically confined Brownian particle in the underdamped case.⁴⁷ More specifically, we have for the optimal driving,

$$F_{opt}(t) = F_{EL}(t) + [x_2(0^+) - x_{20}] \delta(t - 0^+) + [x_{2f} - x_2(t_f^-)] \delta(t - t_f^-). \quad (28)$$

C. Transversality condition for variable end point

Now, we take into account that the final point is not fixed: we only know that it belongs to the limit cycle. Therefore, in the variational procedure, δx_{1f} and δx_{2f} do not vanish and the following condition must hold:

$$0 = \left(\frac{\partial L^*}{\partial \dot{x}_1} \delta x_1 + \frac{\partial L^*}{\partial \dot{x}_2} \delta x_2 \right) \Big|_{t=t_f} = \mathbf{p}_f \cdot \delta \mathbf{x}_f, \quad (29)$$

where $p_{1f} \equiv p_1(t_f)$ and $p_{2f} \equiv p_2(t_f)$. Equation (29) is known as the transversality condition, since it tells us that the vectors \mathbf{p}_f and $\delta \mathbf{x}_f$ are orthogonal—see also the Appendix.

Since the final point belongs to the limit cycle, Eq. (8b) implies that $\delta \mathbf{x}_f$ is parallel to the tangent vector to the phase plane trajectory for the undriven van der Pol equation,

$$\delta \mathbf{x}_f \parallel (f_1(x_{2f}), f_2(x_{1f}, x_{2f}, F = 0)). \quad (30)$$

Recalling that $p_2(t) = 0, \forall t$, the transversality condition tells us that $p_{1f} f_1(x_{2f}) = p_{1f} x_{2f} = 0$. Since $p_1(t)$ is a continuous function of time, $p_{1f} = p_1(t_f^-)$, and making use of Eq. (17), we have

$$2\mu(x_{1f}^2(t_f^-) - 1)x_2(t_f^-)x_{2f} = 0. \quad (31)$$

Note that, as discussed before, the velocity is, in general, discontinuous at the final time; i.e., $x_2(t_f^-) \neq x_{2f}$.

There appear several possibilities:

T1. $x_{2f} = 0$: This condition is only fulfilled at the leftmost and rightmost points of the limit cycle, i.e., $x_{1f} = \pm x_{\ell c}^{\max}$.

T2. $x_2(t_f^-) = 0$: This condition entails, together with Eqs. (16c) and (22), that $C_1 = 0$. This implies that $x_2(t) = 0$ for $t \in (0, t_f)$. In other words, $x_1(t)$ is constant; $x_{10} = x_{1f}$. Clearly, this possibility only makes sense if $x_{10} \in [-x_{\ell c}^{\max}, -1] \cup [+1, +x_{\ell c}^{\max}]$.

T3. $x_{1f} = x_1(t_f^-) = 1$: Again, Eq. (22) implies that $x_1(t)$ is constant, $x_{10} = x_{1f} = 1$, so this possibility is included in T2.

D. Minimum non-conservative work

Taking now into account Eqs. (7), (22), and (25), the non-conservative work W_{nc}^{\min} along the Euler–Lagrange path for a given final point x_{1f} is

$$W_{nc}^{\min} = \mu C_1^2 t_f = \mu \frac{[g(x_{1f}) - g(x_{10})]^2}{4t_f}. \quad (32)$$

To obtain the minimum value of the work, we employ the result obtained from the transversality condition: there are two candidates for the optimal end point: (i) $x_{1f} = \pm x_{\ell c}^{\max}$ and (ii) $x_{1f} = x_{10}$. First, if the point $(x_{10}, 0)$ lies inside the limit cycle, i.e., $|x_{10}| \leq x_{\ell c}^{\max}$, we have that the minimum value of W_{nc} is reached for $x_{1f} = x_{10}$, for which W_{nc}^{\min} vanishes. Second, if the point $(x_{10}, 0)$ lies outside the limit cycle, i.e., $|x_{10}| > x_{\ell c}^{\max}$, we have that the minimum value of W_{nc} is reached at $x_{1f} = \text{sgn}(x_{10})x_{\ell c}^{\max}$.

Therefore, the optimal final position over the limit cycle—in terms of non-conservative work—is the one “closest in x ” to the initial position x_{10} ,

$$x_{1f}^{\text{opt}} = \begin{cases} x_{10} & \text{if } b \leq |x_{10}| \leq x_{\ell c}^{\max}, \\ \text{sgn}(x_{10})x_{\ell c}^{\max} & \text{if } |x_{10}| > x_{\ell c}^{\max}. \end{cases} \quad (33)$$

We have defined $b = 1$ as the position at which the damping force vanishes. We recall that we have assumed $|x_{10}| \geq 1, |x_{1f}| \geq 1$ to minimize W_{nc} . Finally, the minimum non-conservative work to an arbitrary point of the limit cycle is

$$W_{nc}^{\min} = \begin{cases} 0 & \text{if } b \leq |x_{10}| \leq x_{\ell c}^{\max}, \\ \mu \frac{[g(x_{\ell c}^{\max}) - g(|x_{10}|)]^2}{4t_f} & \text{if } |x_{10}| > x_{\ell c}^{\max}. \end{cases} \quad (34)$$

The final expression for the minimum non-conservative work (34) suggests the introduction of a scaled connection time,

$$s_f \equiv t_f/\mu, \quad (35)$$

so that W_{nc}^{\min} can be written as

$$W_{nc}^{\min} = \frac{[g(x_{\ell c}^{\max}) - g(|x_{10}|)]^2}{4s_f} H(|x_{10}| - x_{\ell c}^{\max}), \quad \forall \mu, \quad (36)$$

where $H(x)$ is Heaviside’s step function, $H(x) = 1, \forall x > 0, H(x) = 0, \forall x \leq 0$. In terms of the scaled time s_f , W_{nc}^{\min} still depends on the damping coefficient μ through $x_{\ell c}^{\max}$. This “residual” dependence on μ disappears in the small damping limit; making use of Eq. (11),

we get

$$\tilde{W}_{nc}^{\min} = \frac{[g(\tilde{x}_{lc}^{\max}) - g(|x_{10}|)]^2}{4s_f} H(|x_{10}| - \tilde{x}_{lc}^{\max}), \quad \mu \ll 1. \quad (37)$$

We recall that x_{lc}^{\max} is very close to $\tilde{x}_{lc}^{\max} = 2$ for all μ , the deviation from it being always below 3%.⁴⁴ Therefore, in Sec. III E of physical interpretation of the results, we mainly focus on Eq. (37).

E. Physical interpretation of the results

The minimum non-conservative work \tilde{W}_{nc}^{\min} depends on the initial point $|x_{10}|$ and the scaled connection time $s_f = t_f/\mu$. This is illustrated with the density plot of \tilde{W}_{nc}^{\min} in Fig. 2. We only plot the region $|x_{10}| \geq \tilde{x}_{lc}^{\max}$, because \tilde{W}_{nc}^{\min} identically vanishes for $|x_{10}| < \tilde{x}_{lc}^{\max}$.⁴⁸ A first physical consequence of our result (37) is that \tilde{W}_{nc}^{\min} is proportional to the inverse of the connection time, $\tilde{W}_{nc}^{\min} \propto s_f^{-1}$. In the limit of small damping we are focusing on, the proportionality constant depends only on $|x_{10}|$.⁴⁹ This scaling with the connection time is similar to the one found for the minimum irreversible work for the accelerated connection between equilibrium states of mesoscopic systems in stochastic thermodynamics.^{4,21–24,50}

The dependence of the rhs of \tilde{W}_{nc}^{\min} on the initial position x_{10} is illustrated in Fig. 3 for several values of the scaled connection time s_f . For $|x_{10}| \leq \tilde{x}_{lc}^{\max}$, i.e., when the initial position lies between the extremal positions $\pm \tilde{x}_{lc}^{\max}$ of the limit cycle, W_{nc}^{\min} identically vanishes. For $|x_{10}| > \tilde{x}_{lc}^{\max}$, i.e., when the initial position lies outside the extremal positions of the limit cycle, $W_{nc}^{\min} \neq 0$ and increases with $|x_{10}|$, specifically as $[g(x_{10}) - g(\tilde{x}_{lc}^{\max})]^2$.

Let us now analyze the optimal trajectory and the optimal driving force that lead to the minimum non-conservative work. On the one hand, for $|x_{10}| \leq x_{lc}^{\max}$, $x_{1f}^{\text{opt}} = x_{10}$ and the optimal trajectory leading to the limit cycle corresponds to $C_1 = 0$. Therefore, $x_2 = \dot{x}_1$

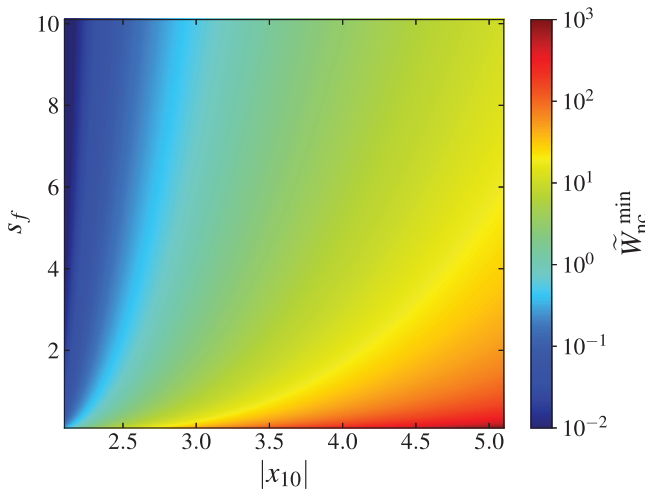


FIG. 2. Minimum non-conservative work \tilde{W}_{nc}^{\min} as a function of scaled connection time s_f and the initial position $|x_{10}|$. The plotted data correspond to the theoretical expression (37) for the small damping limit, which is independent of μ . It is clearly observed how \tilde{W}_{nc}^{\min} decreases as s_f increases and $|x_{10}|$ decreases.

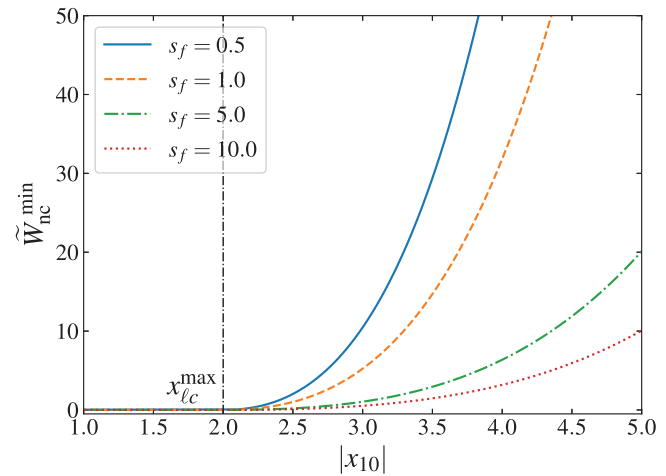


FIG. 3. Non-conservative minimum work \tilde{W}_{nc}^{\min} as a function of $|x_{10}|$. Similar to Fig. 2, the plotted data correspond to the theoretical expression (37). It can be observed that \tilde{W}_{nc}^{\min} increases from zero, for $|x_{10}| \leq \tilde{x}_{lc}^{\max}$, to infinity, in the limit $|x_{10}| \rightarrow +\infty$.

identically vanishes over the optimal solution for $0^+ < t < t_f^-$; the system remains at rest at the point $(x_{10}, 0)$ of the phase plane. The optimal driving force, as given by Eq. (27), is constant, $F_{EL}(t) = x_{10}$. On the other hand, for $|x_{10}| > x_{lc}^{\max}$, $x_{1f}^{\text{opt}} = x_{lc}^{\max}$, and, thus, $C_1 \neq 0$. Since the sign of x_2 , i.e., the sign of \dot{x}_1 , does not change with time and is always that of C_1 , as given by Eq. (22), $x_1(t)$ monotonically varies between x_{10} and x_{1f} . In this case, the optimal driving force (27) is not constant. In both cases, the initial and final values of the velocity are adjusted as we have already commented below in Eq. (27): at $t = 0^+$ and $t = t_f^-$, we introduce two finite-jump discontinuities in the velocity. We recall that this finite-jump discontinuity in the velocity produces no non-conservative work, although they certainly entail that the driving force has delta peaks at the initial and final times, as given by Eq. (28). Note that the only role of the initial velocity x_{20} in the optimal protocol is to modify the correct amplitude for the impulsive contributions to the force, since the Euler-Lagrange solution for $0 < t < t_f$ is blind to the boundary values of x_2 .

Figure 4 shows the optimal trajectory on the phase plane (top panel) and the corresponding optimal force (bottom panel). Specifically, we have employed a damping coefficient $\mu = 0.1$ and a scaled connection time $s_f = 10$, and two initial points on the phase plane: $A_i = (1.5, 0)$ and $B_i = (5, 0)$, which correspond to the two cases discussed in the previous paragraph. For point A_i (dashed lines), there are two equivalent possibilities for the final point, A_f and A'_f , which correspond to driving the system toward the point of the limit cycle just above (red line) or below (blue line) A_i . For point B_i , only one optimal trajectory is possible that ends on the phase plane point $B_f = (x_{lc}^{\max}, 0)$.⁵¹ In the top panel, the arrows mark the direction of movement on the phase plane—recall that $x_2 = \dot{x}_1$. In the bottom panel, the delta peaks of force at the initial and final times are marked with the vertical arrows, which indicate the sign of impulsive forces.

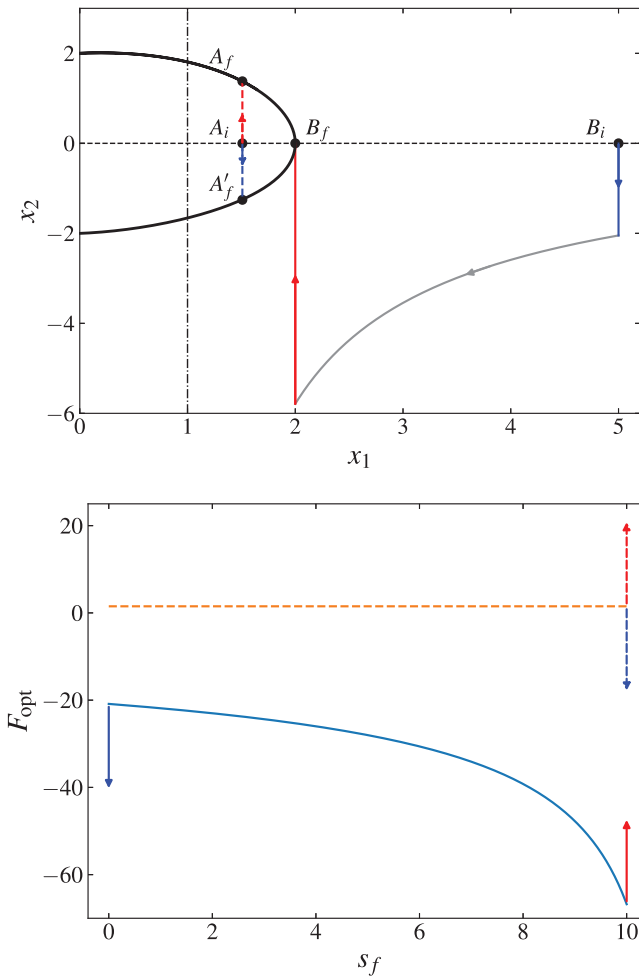


FIG. 4. Optimal phase plane trajectory (top) and force (bottom) for minimizing the non-conservative work. Specifically, a damping constant $\mu = 0.1$ and a scaled connection time $s_f = 10$ have been used. This corresponds to an acceleration factor $t_R/t_f = 40$. Two different values of the initial phase plane point, namely, $A_i = (1.5, 0)$ (dashed lines) and $B_i = (5, 0)$, are considered. The corresponding final points are $A_f \simeq (1.5, 1.4)$, $A'_f \simeq (1.5, -1.3)$, and $B_f \simeq (2, 0)$, respectively. In the top panel, the dotted-dashed vertical line marks the limit of the phase plane region in which the non-conservative work is minimized, i.e., $|x_{10}| > 1$.

Equation (36) entails the emergence of a trade-off relation between connection time t_f and non-conservative work for an accelerated synchronization to the limit cycle. Taking into account that $W_{nc}[\mathbf{x}] \geq W_{nc}^{\min}$, we have, in general,

$$s_f W_{nc}[\mathbf{x}] \geq \frac{[g(x_{lc}^{\max}) - g(|x_{10}|)]^2}{4} H(|x_{10}| - x_{lc}^{\max}), \quad \forall \mu. \quad (38)$$

The monotonic decreasing behavior of W_{nc}^{\min} as a function of connection time entails that there appears a minimum time for the connection for a given value of the non-conservative work W_{nc} . That

is, a speed limit arises,

$$s_f \geq s_f^{\min} = \frac{[g(x_{lc}^{\max}) - g(|x_{10}|)]^2}{4W_{nc}} H(|x_{10}| - x_{lc}^{\max}). \quad (39)$$

In the small damping limit, we have

$$s_f W_{nc}[\mathbf{x}] \geq \frac{[g(\tilde{x}_{lc}^{\max}) - g(|x_{10}|)]^2}{4} H(|x_{10}| - \tilde{x}_{lc}^{\max}), \quad \mu \ll 1. \quad (40)$$

The bound on the rhs is independent of μ , and it only depends on the initial condition x_{10} and remains of the order of unity as long as $|x_{10}| - \tilde{x}_{lc}^{\max} = O(1)$.

IV. GENERALIZATION OF THE RESULTS

A. Liénard equation

The van der Pol equation is a particular case of the Liénard equation,^{18,44,52–57} which we write as

$$\ddot{x} + \mu h(x)\dot{x} + V'(x) = 0, \quad (41)$$

where $h(x)$ and $V(x)$ are even functions of x , $h(x) \in \mathcal{C}^1$ and $V(x) \in \mathcal{C}^2$, respectively. This equation describes a particle moving under the action of a conservative force $-V'(x)$, stemming from a potential energy $V(x)$, and a non-conservative non-linear viscous force $-\mu h(x)\dot{x}$. Equation (41) has a unique stable limit cycle under the following assumptions: (i) $V(x)$ is a confining potential with only one minimum at $x = 0$, and (ii) the function

$$\xi(x) = \int_0^x dx' h(x') \quad (42)$$

has the properties: (a) $\xi(x)$ has only one positive zero at $x = a$, with $\xi(x) < 0$ for $0 < x < a$ and $\xi(x) > 0$ for $x > a$, and (b) $\xi(x)$ is non-decreasing for $x > a$, with $\lim_{x \rightarrow +\infty} \xi(x) = +\infty$.⁵⁸

Remarkably, most of the results for the minimization of the non-conservative work, as derived in Sec. III, also apply to the more general Liénard equation, with small changes. For the Liénard equation, the region in which the non-conservative work can be minimized is defined by the condition $h(x) \geq 0$. Therein, the minimum non-conservative work for a fixed value of x_f is still given by Eq. (32), defining $g(x)$ as the primitive of $\sqrt{h(x)}$, i.e., $g'(x) = \sqrt{h(x)}$. In addition, the optimal final point is given by Eq. (33), with x_{lc}^{\max} being the maximum value of x over the limit cycle. Moreover, this entails that the emergence of a speed limit extends to the Liénard equation. Below, we summarize how these results are derived.

Our starting point is the driven Liénard equation, i.e., we add a force $F(t)$ that we control to its rhs,

$$\ddot{x} + \mu h(x)\dot{x} + V'(x) = F(t), \quad (43)$$

or

$$\dot{x}_1 = \underbrace{x_2}_{f_1}, \quad \dot{x}_2 = \underbrace{-\mu h(x_1)x_2 - V'(x_1) + F}_{f_2}. \quad (44)$$

We assume that $V(x)$ and $h(x)$ verify the conditions under which the undriven Liénard equation has a unique stable limit cycle. Again, we consider the optimal synchronization to this limit cycle, in terms of

the minimum non-conservative work. The work done by the non-conservative viscous force is

$$W_{nc}[\mathbf{x}] = \mu \int_0^{t_f} dt h(x_1) x_2^2. \tag{45}$$

Once more, we would like to minimize the non-conservative work for synchronization to the limit cycle, i.e., we would like to minimize the functional in Eq. (45) with the boundary condition (8)—with $\chi_{\ell c}(\mathbf{x}, \mu) = 0$ standing now for the limit cycle of the Liénard equation.

The above minimization problem can be tackled in the same way as for the van der Pol case, as a variational problem with constraints that can be introduced with the introduction of Lagrange multipliers, the momenta \mathbf{p} . Due to the linearity of f_2 in the force,

$$p_2(t) = 0, \quad p_1(t) = 2\mu h(x_1)x_2, \quad \forall t \in (0, t_f). \tag{46}$$

Taking this into account, we get the Euler–Lagrange equation for the optimal trajectory that minimizes W_{nc} ,

$$2h(x_1)\ddot{x}_1 + h'(x_1)\dot{x}_1^2 = 0. \tag{47}$$

The necessary Clebsch–Legendre condition for having a minimum is now

$$h(x_1) \geq 0. \tag{48}$$

Therefore, for the Liénard equation, we restrict ourselves to the region of the phase plane in which $h(x_1) > 0$. For the sake of simplicity, we consider that there is only one point, $x_1 = b$, at which $h(x_1) = 0$ for $x_1 > 0$. Therefore, Eq. (48) is equivalent to $|x_1| \geq b$; for the van der Pol equation, $b = 1$.

Again, we have a constant of motion,

$$\dot{x}_1 \sqrt{h(x_1)} = C_1. \tag{49}$$

Particularizing this equation to the van der Pol oscillator, where $h(x) = x^2 - 1$, reproduces Eq. (22) of Sec. III. In an analogous way, we find the solution for the optimal trajectory,

$$g'(x) = \sqrt{h(x)} \implies g(x_1) = C_1 t + C_0. \tag{50}$$

Therefore, Eqs. (24) and (25) of Sec. III hold with our redefinition of $g(x)$. The corresponding driving force for the optimal path is

$$F_{EL}(t) = -C_1^2 \frac{h'(x_1)}{2h^2(x_1)} - \mu C_1 \sqrt{h(x_1)} + x_1 \tag{51}$$

for $0^+ < t < t_f^-$. At the initial and final times, two delta peaks are necessary to reach the target values for the initial and final velocities, x_{20} and x_{2f} , as described by Eq. (28).

The transversality condition selects the final point over the limit cycle that gives the minimum non-conservative work. The whole discussion in Sec. III C applies to the Liénard equation, since the explicit shape of the limit cycle was not employed. The unique equation that is specific to the van der Pol equation is (31), since we made use of the particular expression for $p_1(t)$. Yet, the conclusion obtained from it is valid, since for the Liénard equation,

$$p_1(t_f^-) = 2\mu h(x_1(t_f^-))x_2(t_f^-), \tag{52}$$

and, therefore, the transversality condition entails that either $x_2(t_f^-)$ or x_{2f} vanishes.⁵⁹

Equation (32) for the minimum non-conservative work for a fixed final point x_{1f} immediately holds, since Eq. (49) entails that the integrand of W_{nc} equals μC_1^2 over the optimal trajectory. Our discussion on the transversality condition above entails that W_{nc} takes its minimum value at the point x_{1f}^{opt} given by Eq. (33), and Eqs. (34)–(36) also hold for the driven Liénard equation.

The above analysis implies that the scaled time $s = t/\mu$ is also the relevant timescale for the optimal synchronization to the limit cycle in the Liénard equation. In the small damping limit $\mu \ll 1$, the approximate value of the rightmost point of the limit cycle $x_{\ell c}^{max}$ can also be obtained by energetic arguments, similar to those employed for the van der Pol equation: the limit cycle corresponds to a closed orbit $\frac{1}{2}x_2^2 + V(x_1) = E^{(0)}$, where $E^{(0)}$ is determined by imposing that the non-conservative work vanishes over the closed orbit.

B. Minimization of the total work

Let us also consider the minimization of the total work W done by the external force $F(t)$, not only the non-conservative contribution W_{nc} . More precisely, we consider a fixed initial point (x_{10}, x_{20}) on the phase plane and look for (i) the phase plane trajectory $(x_1(t), x_2(t))$ verifying the evolution Eq. (44) and (ii) the final point (x_{1f}, x_{2f}) over the limit cycle that minimizes the total work. Similar to Eq. (6), we have that

$$W = E(x_f) - E(x_0) + W_{nc}[\mathbf{x}], \text{ with } E(\mathbf{x}) \equiv \frac{1}{2}x_2^2 + V(x_1). \tag{53}$$

We consider an infinitesimal variation of the phase plane path $\delta\mathbf{x}$ around the optimal one and impose that the variation of $E(x_f) + W_{nc}[\mathbf{x}]$, with the constraints given by the evolution equation (44) incorporated with the Lagrange multipliers $\mathbf{p}(t)$. The “bulk” term of the variation, for $t \in (0, t_f)$, leads to the Euler–Lagrange equations derived in Sec. III A. For the optimal path verifying the Euler–Lagrange Eq. (47), only the variation at the upper limit survives and must vanish,

$$[\nabla_{x_f} E(x_f) + \mathbf{p}_f] \cdot \delta\mathbf{x}_f = 0, \tag{54}$$

where $\nabla_x E(\mathbf{x}) = (V'(x_1), x_2)$ (see the Appendix for details). Therefore, the *modified transversality condition* (54) tells us that the vector $\nabla_{x_f} E(x_f) + \mathbf{p}_f$ is perpendicular to $\delta\mathbf{x}_f$, which verifies the parallelism condition in Eq. (30). Then, we have

$$\begin{aligned} 0 &= [V'(x_{1f}) + p_{1f}] x_{2f} + x_{2f} [-\mu h(x_1)x_{2f} - V'(x_{1f})] \\ &= x_{2f} [p_1(t_f^-) - \mu h(x_1)x_{2f}] = \mu h(x_1)x_{2f} [2x_2(t_f^-) - x_{2f}]. \end{aligned} \tag{55}$$

Equation (55) has relevant implications. There appear three possibilities:

- MT1. $x_{2f} = 0$: This condition is only fulfilled at the leftmost and rightmost points of the limit cycle, i.e., $x_{1f} = \pm x_{\ell c}^{max}$.
- MT2. $x_2(t_f^-) = x_{2f}/2$: Making use of the first integral (49), together with Eq. (25), we get

$$x_{2f} = \frac{2[g(x_{1f}) - g(x_{10})]}{t_f \sqrt{h(x_{1f})}}, \tag{56}$$

provided that $h(x_{1f}) \neq 0$ (see MT3).

MT3. $h(x_{1f}) = 0$, i.e., $x_{1f} = b$: The first integral (49) tells us that $x_1(t)$ is constant, $x_1(t) = b, \forall t \in [0, t_f]$.

MT1–MT3 are the conditions for the minimization of the total work W corresponding to T1–T3 for the minimization of the non-conservative work. Note that MT3 is no longer a particular case of MT2.

It is interesting to analyze the modified transversality conditions MT1–MT3 in the limit of small damping $\mu \ll 1$, in which the relevant timescale for the connection is $s_f = t_f/\mu$. Therein, Eq. (56) for MT2 is rewritten as

$$\mu x_{2f} = \frac{2[g(x_{1f}) - g(x_{10})]}{s_f \sqrt{h(x_{1f})}}. \tag{57}$$

Note that this is a closed equation for x_{1f} after considering that the final point (x_{1f}, x_{2f}) belongs to the limit cycle, i.e., $\chi_{lc}(x_{1f}, x_{2f}) = 0$. Below, we study the cases corresponding to positions inside the limit cycle, $b \leq |x_{10}| \leq x_{lc}^{max}$, and outside the limit cycle, $|x_{10}| > x_{lc}^{max}$, separately.

First, we consider that the initial position lies inside the limit cycle, $b \leq |x_{10}| \leq x_{lc}^{max}$. Assuming that $x_{2f} = O(1)$, we have that $x_{1f} - x_{10} = O(\mu)$ for $s_f = O(1)$, i.e., we recover to the lowest order, the solution for the non-conservative work. This is reasonable from a physical point of view: for $\mu \ll 1$, the energy is approximately constant—with $O(\mu)$ corrections—over the limit cycle; so minimizing the non-conservative work and the total work is equivalent. (The non-conservative work is of the order of unity for any non-vertical trajectory.) This continues to be true for very short connection times $s_f \ll 1$. Again, this is reasonable: for very short connection times, the non-conservative work diverges for any non-vertical trajectory and dominates the minimization of the total work. Thus, the only exception is the regime of long connection times $s_f \gg 1$, which includes an order of unity times in the original timescale: note that $t_f = 1$ gives $\mu s_f = O(1)$, which would lead to $x_{1f} - x_{10} = O(1)$. For $\mu s_f \gg 1$, $x_{1f} \rightarrow b$ —recall that $h(x_1)$ vanishes at $x_1 = b$.

The above discussion entails that, for initial points inside the limit cycle, $b \leq |x_{10}| \leq x_{lc}^{max}$, we expect the optimal final point to vary with s_f from $x_{1f}^{opt} = x_{10}$ for $s_f \ll 1$ to $x_{1f}^{opt} = b$ for $\mu s_f \gg 1$. In order to check this theoretical prediction, we have employed the particular case of the van der Pol oscillator. In Fig. 5, we plot the total work as a function of the final point x_{1f} (top panel) for different values of the connection time s_f and the corresponding optimal value x_{1f}^{opt} as a function of s_f (bottom panel). Specifically, we have taken $\mu = 0.1$ and $x_{10} = 1.5$. For small values of s_f , the dominance of W_{nc} over ΔE implies that $x_{1f}^{opt} \simeq x_{10}$. As s_f increases, x_{1f}^{opt} starts to decrease until $x_{1f}^{opt} \rightarrow 1$ for $s_f \rightarrow \infty$; recall that $b = 1$ for the van der Pol oscillator. We have numerically checked that x_{1f}^{opt} is accurately determined by condition MT2, i.e., Eq. (57), for all s_f .

We find a different, more complex situation when the initial point lies outside the limit cycle, $|x_{10}| > x_{lc}^{max}$. Figure 6 shows the results for the minimization of the total work, also for the van der Pol oscillator with $\mu = 0.1$ as in Fig. 5 but for $x_{10} = 5$. Again, for small values of s_f , W is dominated by W_{nc} . This entails that the optimal final point is given by condition MT1, i.e., $x_{1f}^{opt} = x_{lc}^{max}$. This situation is maintained until a certain critical value of the connection

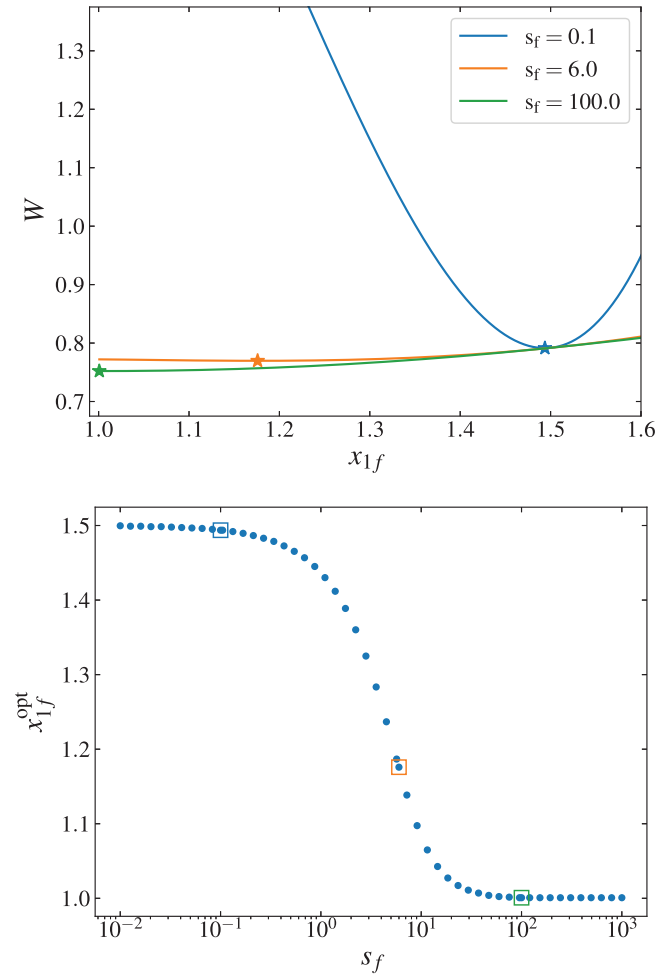


FIG. 5. Total work W as a function of final point over the limit cycle x_{1f} (top) and the optimal final point x_{1f}^{opt} as a function of scaled time s_f (bottom). In particular, the plotted curves correspond to the van der Pol oscillator with a damping constant $\mu = 0.1$, and an initial point inside the limit cycle, namely, $x_{10} = 1.5$. On the top panel, the stars mark the points at which W reaches its minimum as a function of x_{1f} for the considered values of s_f shown in the legend. These points are singled out in the bottom panel with small squares, with the same color code. In the scaled time s , the natural relaxation time here is $s_R = t_R/\mu = 400$.

time, $s_f = s_f^*$, is reached. Thereat, x_{1f}^{opt} abruptly changes and from that moment on is given by condition MT2, i.e., Eq. (57). This sudden change can be explained by taking a look at the top plot of Fig. 6. When s_f is long enough, W has a local minimum given by Eq. (57). This local minimum may be the global one depending on the value of W at its boundary $x_{1f} = x_{lc}^{max}$. There is a critical value of the connection time $s_f = s_f^*$ where both values equate. For shorter times, $x_{1f}^{opt} = x_{lc}^{max}$, whereas for longer times, the optimal point for synchronization is provided by Eq. (57). Note that for $s_f > s_f^*$, the behavior is identical to the previous case, x_{1f}^{opt} asymptotically tends to $b = 1$ in the limit as $s_f \rightarrow \infty$.

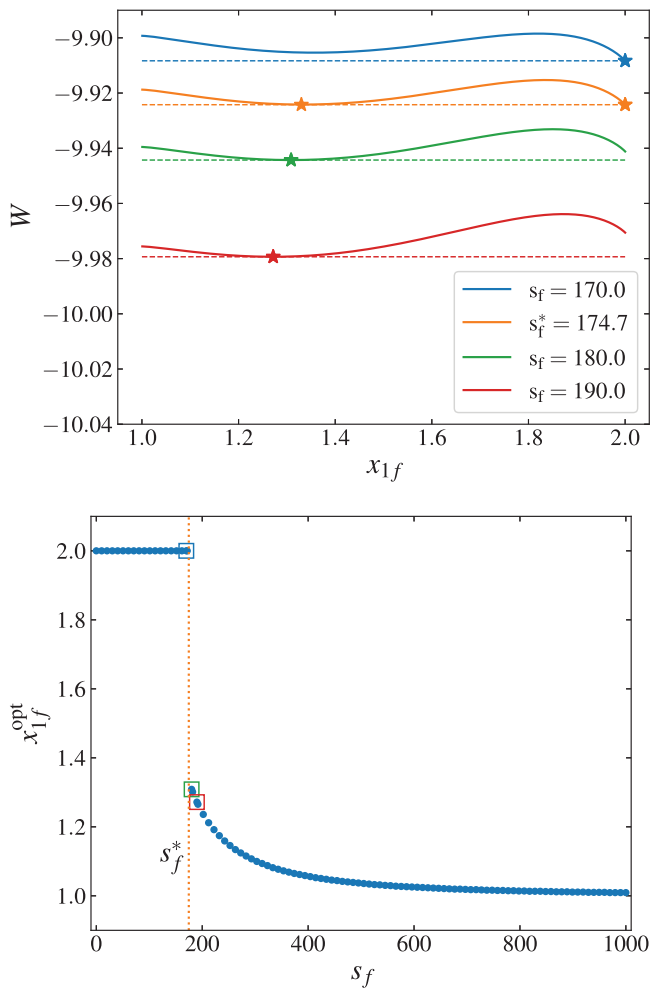


FIG. 6. Total work W as a function of final point over the limit cycle (top) and the optimal final limit cycle point x_{1f}^{opt} as a function of scaled time s_f . Again, the plotted curves correspond to the van der Pol oscillator with a damping constant $\mu = 0.1$, but the initial point lies outside the limit cycle, namely, $x_{10} = 5$. The code for the stars (top) and the small squares (bottom) is analogous to that in Fig. 5. At $s_f = s_f^* \simeq 174.7$, it can be observed how the local minimum of W equals its value at the boundary $x_{1f} = x_{lc}^{max}$.

V. CONCLUSIONS AND PERSPECTIVES

In this work, we have investigated the optimal synchronization of the van der Pol oscillator to its limit cycle. We have understood optimality in terms of the minimization of the non-conservative work from a given initial point $\mathbf{x}_0 = (x_{10}, x_{20})$ on the phase plane to any final point $\mathbf{x}_f = (x_{1f}, x_{2f})$ belonging to the limit cycle, in a given connection time t_f . The non-conservative work can be minimized if both the initial and final points lie on the same region of the phase plane where the non-conservative force is dissipative, i.e., $|x_1| \geq 1$. Interestingly, the minimum non-conservative work W_{nc}^{min} depends on the initial position x_{10} but not on the initial velocity x_{20} .

The minimization of the non-conservative work has some interesting physical consequences. For initial points such that its initial position x_{10} lies “inside” the limit cycle, i.e., $|x_{10}| \leq x_{lc}^{max}$, the minimum conservative work corresponds to a vertical trajectory in phase space with a constant position, $x_1(t) = x_{10}$, and zero velocity, $x_2(t) = 0$, and, thus, zero non-conservative work. The final point over the limit cycle is reached by introducing a delta-peak force, i.e., an impulsive force that instantaneously changes the velocity without altering the position. For initial points such that its initial position x_{10} lies “outside” the limit cycle, i.e., $|x_{10}| > x_{lc}^{max}$, the optimal phase-space trajectory joins the initial point with the rightmost or leftmost point of the limit cycle ($\pm x_{lc}^{max}, 0$), depending on the sign of x_{10} . Analogous to recent results for the irreversible work in the field of stochastic thermodynamics, the minimum non-conservative work in this case is inversely proportional to the connection time. This implies that there appears a speed-limit inequality for the synchronization to the limit cycle.

Especially interesting is the small damping limit $\mu \ll 1$, in which the natural relaxation time t_R to the limit cycle is very long, $t_R = O(\mu^{-1})$. Therein, the speed-limit inequality reads $s_f W_{nc} \geq I_0$, where I_0 is an order of unity bound—which only depends on the initial point—and $s_f = t_f/\mu$ is a scaled connection time. This speed-limit inequality entails that a SST transformation with a very short connection time, $s_f = t_f/\mu = O(1)$, can be done with finite cost. Note that the acceleration obtained in this case is enormous, $t_f/t_R = O(\mu^2)$.

It is remarkable that most of the results for the van der Pol oscillator extend to the Liénard equation, including the t_f^{-1} dependence of the non-conservative work and, thus, the emergence of a speed-limit inequality. It is also interesting that the optimality of the rightmost/leftmost points of the limit cycle—in terms of minimizing the non-conservative work for the synchronization thereto—can also be established for the Liénard equation. This property follows from purely geometric arguments, stemming from the transversality condition, without needing to have a closed expression for the limit cycle.

We have also considered the problem of minimizing the total work done by the external force, including both conservative and non-conservative contributions thereto. From the point of view of SST, the most relevant regime is that of small damping $\mu \ll 1$ with an order of unity scaled connection time s_f —which, as stated above, imply an enormous acceleration of the dynamics; the acceleration factor diverges as μ^{-2} . Therein, the minimization of the total work W is dominated by the non-conservative contribution W_{nc} , and, therefore, the optimal final point over the limit cycle coincides—to the lowest order—with that obtained for W_{nc} . As the connection time s_f increases, the non-conservative contribution to the work decreases and there appears a competition with the conservative contribution—which is expressed mathematically by the modified transversality condition MT2 [Eq. (57)]. For initial points inside the limit cycle, $|x_{10}| \leq x_{lc}^{max}$, the optimal final point smoothly varies from $x_{1f}^{opt} = x_{10}$ for $s_f \ll 1$ to $x_{1f} = 1$ for $\mu s_f \gg 1$. For initial points outside the limit cycle, $|x_{10}| > x_{lc}^{max}$, the behavior of the optimal final point is more complex: there appears a critical value s_f^* , at which x_{1f}^{opt} presents a jump discontinuity, but the minimum work is continuous. Therefore, this is analogous to a first-order phase transition,

with the optimal final point x_{1f}^{opt} playing the role of an order parameter. For $s_f < s_f^*$, $x_{1f}^{\text{opt}} = x_{1c}^{\text{max}}$, as was the case for the non-conservative work, whereas x_{1f}^{opt} follows Eq. (57) for $s_f > s_f^*$.

Non-linear systems typically call for specific approaches, almost always involving approximations—e.g., there is not a general theory for solving non-linear differential equations, in contrast with the situation for the linear case. Nevertheless, we have been able here to derive a whole framework for the minimization of the work done in the synchronization to a limit cycle in a general class of non-linear systems, with many exact analytical results—without knowing the explicit function that gives the shape of the limit cycle. This is a remarkable result, which may pave the way to find the optimal synchronization to self-sustained oscillations in more complex non-linear systems, which are relevant in many fields such as active matter and other biological contexts.^{7–10,13,60–62}

From a practical point of view, there is a maximum value of the force that can be applied, i.e., $|F(t)| \leq K$, in any actual physical system. Moreover, the force can only be applied during a non-vanishing time interval. Hence, it would be interesting to address the minimization of the work with the non-holonomic constraint $|F(t)| \leq K$ —which makes it necessary to resort to the tools of optimal control theory, specifically Pontryagin's maximum principle.^{40,63} For large enough K , physical intuition makes one expect a regularized version of Eq. (28) as the solution of the optimal control, with (i) the initial and final delta peaks being substituted with very short—as compared to the smallest intrinsic timescale of the undriven system—time windows where $F(t) = \pm K$, and (ii) an intermediate time window, between the short initial and final ones, in which the solution follows the Euler–Lagrange equations.⁶⁴ The expectation of the three-stage picture just described is based on the position of the particle being changed by a tiny, infinitesimal from a mathematical point of view, amount in the initial and final time windows—i.e., for a large enough K , the initial and final $\pm K$ forces are impulsive within a high degree of approximation. As K is decreased, the duration of the necessary initial and final time windows increase and become comparable to the intrinsic timescales, making the position appreciably change therein. As a consequence, the validity of the simple three-stage picture outlined above cannot be guaranteed as K decreases, and a thorough analysis of the constrained control problem becomes compulsory.

ACKNOWLEDGMENTS

C.R.-M., C.A.P., and A.P. acknowledge financial support through Grant No. PID2021-122588NB-I00 funded by MCIN/AEI/10.13039/501100011033/ and by “ERDF A way of making Europe.” All authors acknowledge financial support from Grant ProyExcel_00796 funded by Junta de Andalucía's PAIDI 2020 program. C.A.P. acknowledges the funding received from the European Union's Horizon Europe–Marie Skłodowska-Curie 2021 program through the Postdoctoral Fellowship Reference No. 101065902 (ORION). C.R.-M. acknowledges support from the Ministry of Science, Innovation and Universities FPU program through Grant No. FPU22/01151.

AUTHOR DECLARATIONS

Conflict of Interest

The authors have no conflicts to disclose.

Author Contributions

C. Ríos-Monje: Conceptualization (equal); Data curation (equal); Formal analysis (equal); Investigation (equal); Methodology (equal); Validation (equal); Visualization (equal); Writing – original draft (equal); Writing – review & editing (equal). **C. A. Plata:** Conceptualization (equal); Data curation (equal); Formal analysis (equal); Investigation (equal); Methodology (equal); Validation (equal); Visualization (equal); Writing – original draft (equal); Writing – review & editing (equal). **D. Guéry-Odelin:** Conceptualization (equal); Data curation (supporting); Formal analysis (equal); Investigation (equal); Methodology (equal); Validation (equal); Visualization (equal); Writing – original draft (equal); Writing – review & editing (equal). **A. Prados:** Conceptualization (equal); Formal analysis (equal); Funding acquisition (lead); Investigation (equal); Methodology (equal); Supervision (lead); Validation (equal); Visualization (equal); Writing – original draft (equal); Writing – review & editing (equal).

DATA AVAILABILITY

The Python codes employed for generating the data and figures that support the findings of this study are openly available in the [GitHub page](#) of University of Sevilla's FINE research group.

APPENDIX A: TRANSVERSALITY CONDITION

In this [Appendix](#), we look into a detailed derivation of the transversality condition in a general case. Let $\mathbf{x} : [t_0, t_f] \rightarrow \mathbb{R}^n$ be a $\mathcal{C}^1(t_0, t_f)$ function representing the phase space trajectory of a system. Now, let us consider the “cost” functional $S[\mathbf{x}]$ of a given trajectory \mathbf{x} . We assume this cost to have the general form

$$S[\mathbf{x}] = \int_{t_0}^{t_f} dt L(\mathbf{x}, \dot{\mathbf{x}}) + M(\mathbf{x}_f), \quad (\text{A1})$$

i.e., $L(\mathbf{x}, \dot{\mathbf{x}})$ is the “Lagrangian” of the problem, the time integral of which provides the running cost during the interval $(0, t_f)$, whereas $M(\mathbf{x}_f)$ is a \mathcal{C}^1 function giving the terminal cost of the trajectory, with $\mathbf{x}_f \equiv \mathbf{x}(t_f)$.

Now, we consider the minimization problem,

$$\min_{\mathbf{x} \in \mathcal{C}^1(t_0, t_f)} S[\mathbf{x}], \quad (\text{A2})$$

which is known in optimal control theory as the Bolza problem.⁴⁰ For our purposes, we analyze the Bolza problem subject to the boundary conditions,

$$\mathbf{x}(t_0) = \mathbf{x}_0, \quad g(\mathbf{x}_f) = 0, \quad (\text{A3})$$

where g is a given function. That is, the initial point is fixed, while the final point lies on a certain target set $g(\mathbf{x}_f) = 0$.

The first-order necessary condition for optimality is $\delta S = 0$. Since \mathbf{x}_0 is fixed, $\delta \mathbf{x}_0 = 0$. This means

$$\delta S = \int_{t_0}^{t_f} dt [\delta \mathbf{x} \cdot \nabla_{\mathbf{x}} L(\mathbf{x}, \dot{\mathbf{x}}) + \delta \dot{\mathbf{x}} \cdot \nabla_{\dot{\mathbf{x}}} L(\mathbf{x}, \dot{\mathbf{x}})] + \delta \mathbf{x}_f \cdot \nabla_{\mathbf{x}_f} M(\mathbf{x}_f) = 0. \quad (\text{A4})$$

Integrating, by parts, the second term of the integral, we get

$$\delta S = \int_{t_0}^{t_f} dt \delta \mathbf{x} \cdot \left[\nabla_{\mathbf{x}} L(\mathbf{x}, \dot{\mathbf{x}}) - \frac{d}{dt} \nabla_{\dot{\mathbf{x}}} L(\mathbf{x}, \dot{\mathbf{x}}) \right] + \delta \mathbf{x}_f \cdot \left[\mathbf{p}_f + \nabla_{\mathbf{x}_f} M(\mathbf{x}_f) \right] = 0, \quad (\text{A5})$$

where we have defined the momenta and its final value as

$$\mathbf{p} \equiv \nabla_{\dot{\mathbf{x}}} L(\mathbf{x}, \dot{\mathbf{x}}), \quad \mathbf{p}_f \equiv \mathbf{p}(t_f). \quad (\text{A6})$$

If \mathbf{x}_f were fixed—as is the case in the least action principle of classical mechanics,⁶⁵ the last term of Eq. (A5) would identically vanish. Then, the arbitrariness of $\delta \mathbf{x}(t)$ in the time interval $(0, t_f)$ leads to the Euler–Lagrange equation,

$$\nabla_{\mathbf{x}} L(\mathbf{x}, \dot{\mathbf{x}}) - \frac{d}{dt} \nabla_{\dot{\mathbf{x}}} L(\mathbf{x}, \dot{\mathbf{x}}) = \mathbf{0}. \quad (\text{A7})$$

In our case, \mathbf{x}_f is not fixed, and it lies on the curve $g(\mathbf{x}_f) = 0$. Yet, since $\delta \mathbf{x}(t)$ for $t \in (0, t_f)$ and $\delta \mathbf{x}_f$ can be independently varied, (i) the Euler–Lagrange equations continue to hold and (ii) the boundary term in Eq. (A5) must also vanish, i.e.,

$$\delta \mathbf{x}_f \cdot \left[\mathbf{p}_f + \nabla_{\mathbf{x}_f} M(\mathbf{x}_f) \right] = 0. \quad (\text{A8})$$

This condition is known as the transversality condition, since it tells us that $\mathbf{p}_f + \nabla_{\mathbf{x}_f} M(\mathbf{x}_f)$ must be orthogonal to $\delta \mathbf{x}_f$. It selects, among all the points on the target set $g(\mathbf{x}_f) = 0$, the optimal final point.

In the main text, we have first considered the problem of the minimization of the non-conservative work. In that case, there is no terminal cost and the transversality condition reduces to $\delta \mathbf{x}_f \cdot \mathbf{p}_f = 0$, Eq. (29). Later, we have considered the problem of minimizing the total work. The inclusion of the conservative contribution thereto entails that there is now a terminal cost $E(\mathbf{x}_f)$, as expressed by Eq. (53). The transversality condition, thus, changes to $\delta \mathbf{x}_f \cdot \left[\mathbf{p}_f + \nabla_{\mathbf{x}_f} E(\mathbf{x}_f) \right] = 0$ [Eq. (54)]. It is to differentiate Eq. (54) from Eq. (29) that we have referred to the former as the modified transversality condition in this paper.

REFERENCES

- ¹J.-M. Ginoux and C. Letellier, “Van der Pol and the history of relaxation oscillations: Toward the emergence of a concept,” *Chaos* **22**, 023120 (2012).
- ²A. Jenkins, “Self-oscillation,” *Phys. Rep.* **525**, 167–222 (2013).
- ³D. Guéry-Odelin, A. Ruschhaupt, A. Kiely, E. Torrontegui, S. Martínez-Garaot, and J. G. Muga, “Shortcuts to adiabaticity: Concepts, methods, and applications,” *Rev. Mod. Phys.* **91**, 045001 (2019).
- ⁴D. Guéry-Odelin, C. Jarzynski, C. A. Plata, A. Prados, and E. Trizac, “Driving rapidly while remaining in control: Classical shortcuts from Hamiltonian to stochastic dynamics,” *Rep. Prog. Phys.* **86**, 035902 (2023).
- ⁵B. van der Pol, “LXXXVIII. On “relaxation-oscillations,”” *London Edinburgh Dublin Philos. Mag. J. Sci.* **2**, 978–992 (1926).

- ⁶H. Sakaguchi, “Limit-cycle oscillation of an elastic filament and caterpillar motion,” *Phys. Rev. E* **79**, 026216 (2009).
- ⁷R. Allicki, D. Gelbwaser-Klimovsky, and A. Jenkins, “Leaking elastic capacitor as model for active matter,” *Phys. Rev. E* **103**, 052131 (2021).
- ⁸T. Kotwal, F. Moseley, A. Stegmaier, S. Imhof, H. Brand, T. Kießling, R. Thomale, H. Ronellenfitch, and J. Dunkel, “Active topoelectrical circuits,” *Proc. Natl. Acad. Sci. U.S.A.* **118**, e2106411118 (2021).
- ⁹S. Liu, S. Shankar, M. C. Marchetti, and Y. Wu, “Viscoelastic control of spatiotemporal order in bacterial active matter,” *Nature* **590**, 80–84 (2021).
- ¹⁰G. Tucci, E. Roldán, A. Gambassi, R. Belousov, F. Berger, R. Alonso, and A. Hudspeth, “Modeling active non-Markovian oscillations,” *Phys. Rev. Lett.* **129**, 030603 (2022).
- ¹¹J.-C. Leloup, D. Gonze, and A. Goldbeter, “Limit cycle models for circadian rhythms based on transcriptional regulation in *Drosophila* and *Neurospora*,” *J. Biol. Rhythms* **14**, 433–448 (1999).
- ¹²T. Roenneberg, E. J. Chua, R. Bernardo, and E. Mendoza, “Modelling biological rhythms,” *Curr. Biol.* **18**, R826–R835 (2008).
- ¹³D. B. Brückner, A. Fink, C. Schreiber, P. J. F. Röttgermann, J. O. Rädler, and C. P. Broedersz, “Stochastic nonlinear dynamics of confined cell migration in two-state systems,” *Nat. Phys.* **15**, 595–601 (2019).
- ¹⁴R. FitzHugh, “Impulses and physiological states in theoretical models of nerve membrane,” *Biophys. J.* **1**, 445–466 (1961).
- ¹⁵J. Nagumo, S. Arimoto, and S. Yoshizawa, “An active pulse transmission line simulating nerve axon,” *Proc. IRE* **50**, 2061–2070 (1962).
- ¹⁶J. H. E. Cartwright, V. M. Eguiluz, E. Hernández-García, and O. Piro, “Dynamics of elastic excitable media,” *Int. J. Bifurcation Chaos* **09**, 2197–2202 (1999).
- ¹⁷P. Romanczuk, M. Bär, W. Ebeling, B. Lindner, and L. Schimansky-Geier, “Active Brownian particles: From individual to collective stochastic dynamics,” *Eur. Phys. J. Spec. Top.* **202**, 1–162 (2012).
- ¹⁸S. H. Strogatz, *Nonlinear Dynamics and Chaos: With Applications to Physics, Biology, Chemistry, and Engineering*, 3rd ed. (Chapman and Hall, Boca Raton, 2024).
- ¹⁹F. Impens and D. Guéry-Odelin, “Shortcut to synchronization in classical and quantum systems,” *Sci. Rep.* **13**, 453 (2023).
- ²⁰T. Schmiedl and U. Seifert, “Optimal finite-time processes in stochastic thermodynamics,” *Phys. Rev. Lett.* **98**, 108301 (2007).
- ²¹E. Aurell, C. Mejía-Monasterio, and P. Muratore-Ginanneschi, “Optimal protocols and optimal transport in stochastic thermodynamics,” *Phys. Rev. Lett.* **106**, 256001 (2011).
- ²²C. A. Plata, D. Guéry-Odelin, E. Trizac, and A. Prados, “Optimal work in a harmonic trap with bounded stiffness,” *Phys. Rev. E* **99**, 012140 (2019).
- ²³Y. Zhang, “Work needed to drive a thermodynamic system between two distributions,” *Europhys. Lett.* **128**, 30002 (2020).
- ²⁴D. A. Sivak and G. E. Crooks, “Thermodynamic metrics and optimal paths,” *Phys. Rev. Lett.* **108**, 190602 (2012).
- ²⁵S. Deffner and S. Campbell, “Quantum speed limits: From Heisenberg’s uncertainty principle to optimal quantum control,” *J. Phys. A: Math. Theor.* **50**, 453001 (2017).
- ²⁶M. Okuyama and M. Ohzeki, “Quantum speed limit is not quantum,” *Phys. Rev. Lett.* **120**, 070402 (2018).
- ²⁷N. Shiraishi, K. Funo, and K. Saito, “Speed limit for classical stochastic processes,” *Phys. Rev. Lett.* **121**, 070601 (2018).
- ²⁸B. Shanahan, A. Chenu, N. Margolus, and A. del Campo, “Quantum speed limits across the quantum-to-classical transition,” *Phys. Rev. Lett.* **120**, 070401 (2018).
- ²⁹K. Funo, N. Shiraishi, and K. Saito, “Speed limit for open quantum systems,” *New J. Phys.* **21**, 013006 (2019).
- ³⁰N. Shiraishi and K. Saito, “Speed limit for open systems coupled to general environments,” *Phys. Rev. Res.* **3**, 023074 (2021).
- ³¹C. A. Plata, D. Guéry-Odelin, E. Trizac, and A. Prados, “Finite-time adiabatic processes: Derivation and speed limit,” *Phys. Rev. E* **101**, 032129 (2020).
- ³²S. Deffner, “Quantum speed limits and the maximal rate of information production,” *Phys. Rev. Res.* **2**, 013161 (2020).
- ³³S. Ito and A. Dechant, “Stochastic time-evolution, information geometry and the Cramer-Rao bound,” *Phys. Rev. X* **10**, 021056 (2020).
- ³⁴T. Van Vu and Y. Hasegawa, “Geometrical bounds of the irreversibility in Markovian systems,” *Phys. Rev. Lett.* **126**, 010601 (2021).

- ³⁵A. Prados, “Optimizing the relaxation route with optimal control,” *Phys. Rev. Res.* **3**, 023128 (2021).
- ³⁶J. S. Lee, S. Lee, H. Kwon, and H. Park, “Speed limit for a highly irreversible process and tight finite-time Landauer’s bound,” *Phys. Rev. Lett.* **129**, 120603 (2022).
- ³⁷A. Patrón, A. Prados, and C. A. Plata, “Thermal brachistochrone for harmonically confined Brownian particles,” *Eur. Phys. J. Plus* **137**, 1011 (2022).
- ³⁸A. Dechant, “Minimum entropy production, detailed balance and Wasserstein distance for continuous-time Markov processes,” *J. Phys. A: Math. Theor.* **55**, 094001 (2022).
- ³⁹I. M. Gelfand and S. V. Fomin, *Calculus of Variations* (Dover Publications, 2000).
- ⁴⁰D. Liberzon, *Calculus of Variations and Optimal Control Theory: A Concise Introduction* (Princeton University Press, 2012).
- ⁴¹Note that, at variance with simpler problems with linear damping, the sign of W_{nc} is not fixed because the factor $x_1^2 - 1$ changes sign at $x_1 = 1$.
- ⁴²S. Blaber and D. A. Sivak, “Optimal control in stochastic thermodynamics,” *J. Phys. Commun.* **7**, 033001 (2023).
- ⁴³For fixed initial and final points of the trajectory on phase plane, ΔE has a given value. In that case, the problem of minimizing the non-conservative work W_{nc} and the total work done by the external force $F(t)$ are always equivalent. See also Sec. IV B.
- ⁴⁴N. Turner, P. V. E. McClintock, and A. Stefanovska, “Maximum amplitude of limit cycles in Liénard systems,” *Phys. Rev. E* **91**, 012927 (2015).
- ⁴⁵Note that this definition of H , which is the one employed in classical mechanics, leads to the usual definition in Pontryagin’s theory of optimal control.
- ⁴⁶H. M. Robbins, “A generalized Legendre-Clebsch condition for the singular cases of optimal control,” *IBM J. Res. Dev.* **11**, 361–372 (1967).
- ⁴⁷A. Gomez-Marín, T. Schmiedl, and U. Seifert, “Optimal protocols for minimal work processes in underdamped stochastic thermodynamics,” *J. Chem. Phys.* **129**, 024114 (2008).
- ⁴⁸Due to the symmetry $x_1 \rightarrow -x_1$ of our problem, all plots in this section are for $|x_{10}| \geq 1$.
- ⁴⁹For an arbitrary value of μ , the proportionality constant also depends very weakly on the damping coefficient μ through x_{tc}^{\max} .
- ⁵⁰C. A. Plata, A. Prados, E. Trizac, and D. Guéry-Odelin, “Taming the time evolution in overdamped systems: Shortcuts elaborated from fast-forward and time-reversed protocols,” *Phys. Rev. Lett.* **127**, 190605 (2021).
- ⁵¹For $\mu = 0.1$, $x_{tc}^{\max} = 2.000\ 10$.⁴⁴
- ⁵²R. Iacono and F. Russo, “Class of solvable nonlinear oscillators with isochronous orbits,” *Phys. Rev. E* **83**, 027601 (2011).
- ⁵³M. Messias and M. R. Alves Gouveia, “Time-periodic perturbation of a Liénard equation with an unbounded homoclinic loop,” *Physica D* **240**, 1402–1409 (2011).
- ⁵⁴S. Ghosh and D. S. Ray, “Liénard-type chemical oscillator,” *Eur. Phys. J. B* **87**, 65 (2014).
- ⁵⁵T. Shah, R. Chattopadhyay, K. Vaidya, and S. Chakraborty, “Conservative perturbation theory for nonconservative systems,” *Phys. Rev. E* **92**, 062927 (2015).
- ⁵⁶J. Giné, “Liénard equation and its generalizations,” *Int. J. Bifurcation Chaos* **27**, 1750081 (2017).
- ⁵⁷A. Mishra, S. Saha, and S. K. Dana, “Chimeras in globally coupled oscillators: A review,” *Chaos* **33**, 092101 (2023).
- ⁵⁸For the van der Pol equation, $\xi(x) = (x^3 - 3x)/3$ and $a = \sqrt{3}$.
- ⁵⁹Similarly to the discussion below Eq. (31), the case $h(x_1(t_f^-)) = 0$ is a particular case of $x_2(t_f^-) = 0$.
- ⁶⁰Z. Hu, Y. Li, and J.-A. Lv, “Phototunable self-oscillating system driven by a self-winding fiber actuator,” *Nat. Commun.* **12**, 3211 (2021).
- ⁶¹J. Landman, S. M. Verduyn Lunel, and W. K. Kegel, “Transcription factor competition facilitates self-sustained oscillations in single gene genetic circuits,” *PLoS Comput. Biol.* **19**, e1011525 (2023).
- ⁶²E. Zheng, M. Brandenbourger, L. Robinet, P. Schall, E. Lerner, and C. Coulais, “Self-oscillation and synchronization transitions in elastoactive structures,” *Phys. Rev. Lett.* **130**, 178202 (2023).
- ⁶³L. S. Pontryagin, *Mathematical Theory of Optimal Processes* (CRC Press, 1987).
- ⁶⁴In fact, this is the case for other underdamped control problems, see, for instance, Ref. 66.
- ⁶⁵L. D. Landau and E. M. Lifshitz, “Course of theoretical physics: Vol. 1, Mechanics,” in *Course of Theoretical Physics*, 3rd ed. (Butterworth-Heinemann, 1976).
- ⁶⁶M. Baldovin, I. B. Yedder, C. A. Plata, D. Raynal, L. Rondin, E. Trizac, and A. Prados, “Optimal control of levitated nanoparticles through finite-stiffness confinement,” *arXiv:2408.00043* (2024).